The interplay between tissue-resident microbiome and host proteins by integrated multi-omics during progression of colorectal adenoma to carcinoma

Di Wu[1#], An-Jun Wang[1#], De-Chao Bu[2#], Yan-Yan Sun[1#], Chen-Hao Li[2#], Yue-Mei Hong[1], Shan Zhang[2], Shi-Yang Chen[3], Jin-An Zhou[1],Tian-Yi Zhang[1], Min-Hao Yu[4], Yong-Jing Ma[1], Xiu-Li Wang[1], Jia Xu[4], Wei He[4], Christopher Heeschen[1], Jian-Feng Chen[3,5], Wen-Jun Mao[6*], Hui Ding[4*], Wen-Juan Wu[7*], Yi Zhao[2*], Hui Wang[1*], Ning-Ning Liu[1*]

[1]School of Public Health, Shanghai Jiao Tong University School of Medicine, Shanghai, China.
[2]Institute of Computing Technology, Chinese Academy of Sciences, Beijing, China.
[3]Hangzhou Institute for Advanced Study, University of Chinese Academy of Sciences, Hangzhou 310024, China
[4]Renji Hospital, Shanghai Jiao Tong University School of Medicine, Shanghai, China.
[5]School of Basic Medical Sciences, Fudan University, Shanghai 200032, China.
[6]The Affiliated Wuxi People's Hospital of Nanjing Medical University, Wuxi , China.
[7]Shanghai East Hospital, Tongji University School of Medicine, Shanghai, China.

Di Wu, An-Jun Wang, De-Chao Bu, Yan-Yan Sun, Chen-Hao Li, Yue-Mei Hong, Shan Zhang, et al. 2025. The Interplay Between Tissue-Resident Microbiome and Host Proteins by Integrated Multi-omics During Progression of Colorectal Adenoma to Carcinoma. ***iMeta*** 4: e70090. https://doi.org/10.1002/imt2.70090

Introduction

Absolute numbers, Incidence, Both sexes, in 2022

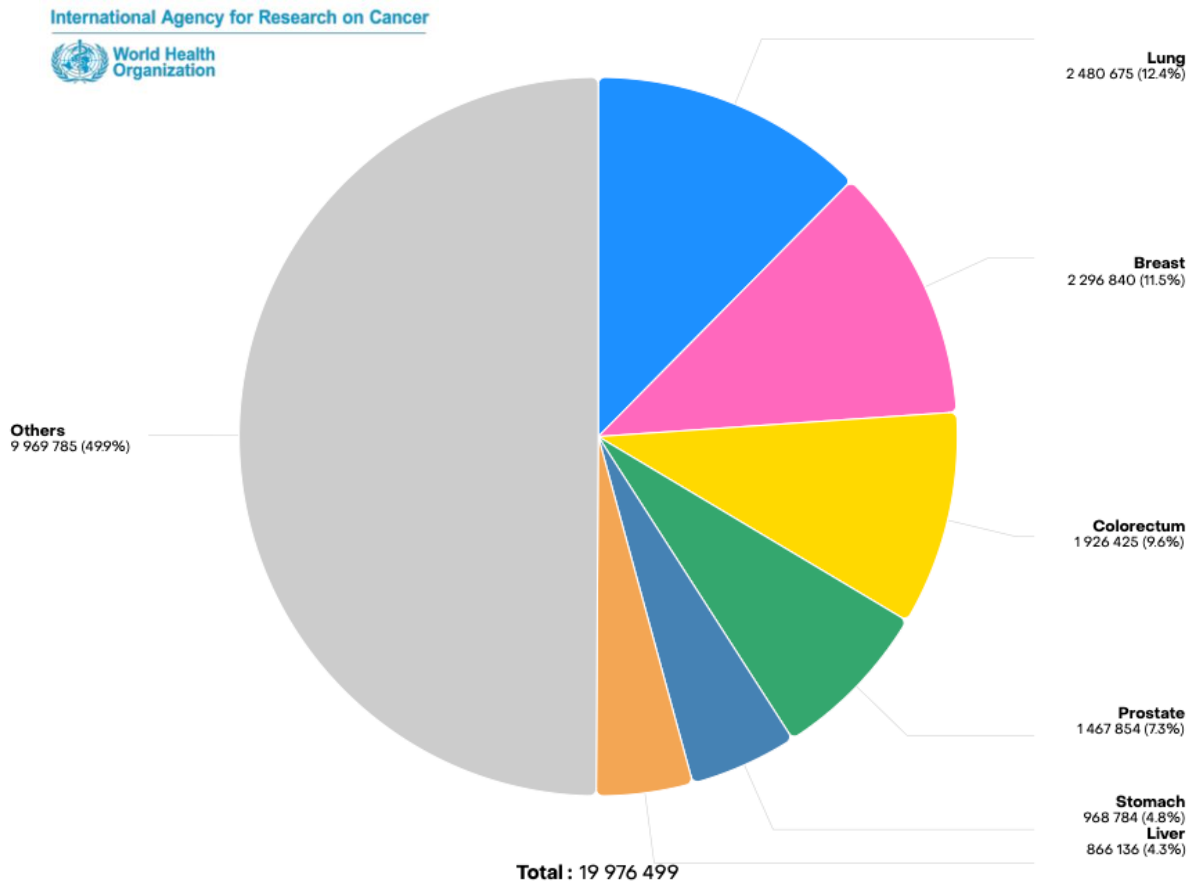

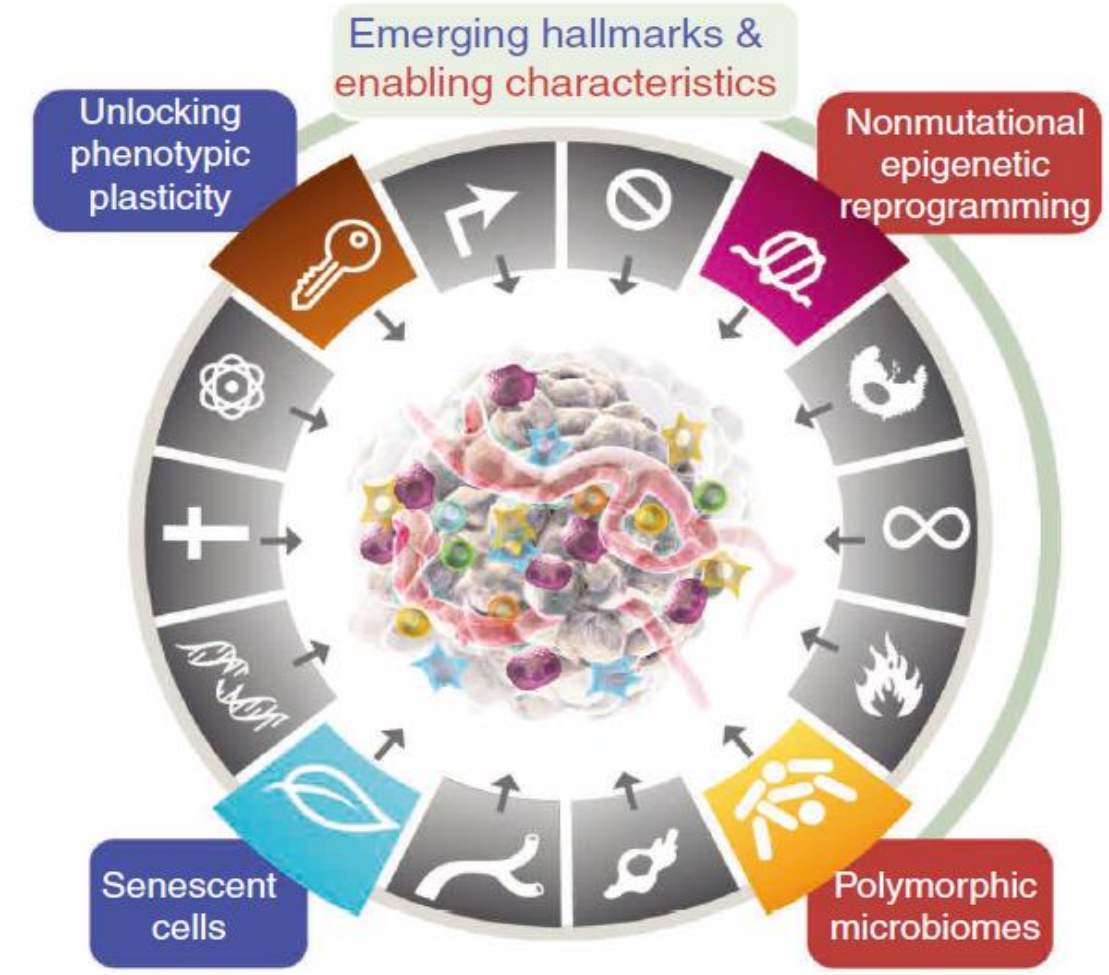

Douglas Hanahan, *Cancer Discovery*, 2022

- Colorectal cancer (CRC) is the 3rd most common cancer worldwide, high mortality.
- Early detection drastically improves survival.

- Intratumoral microbiome is an emerging hallmark of cancer.
- Its multi-kingdom host–microbiome ecosystem in CRC remains poorly characterized.

Highlights

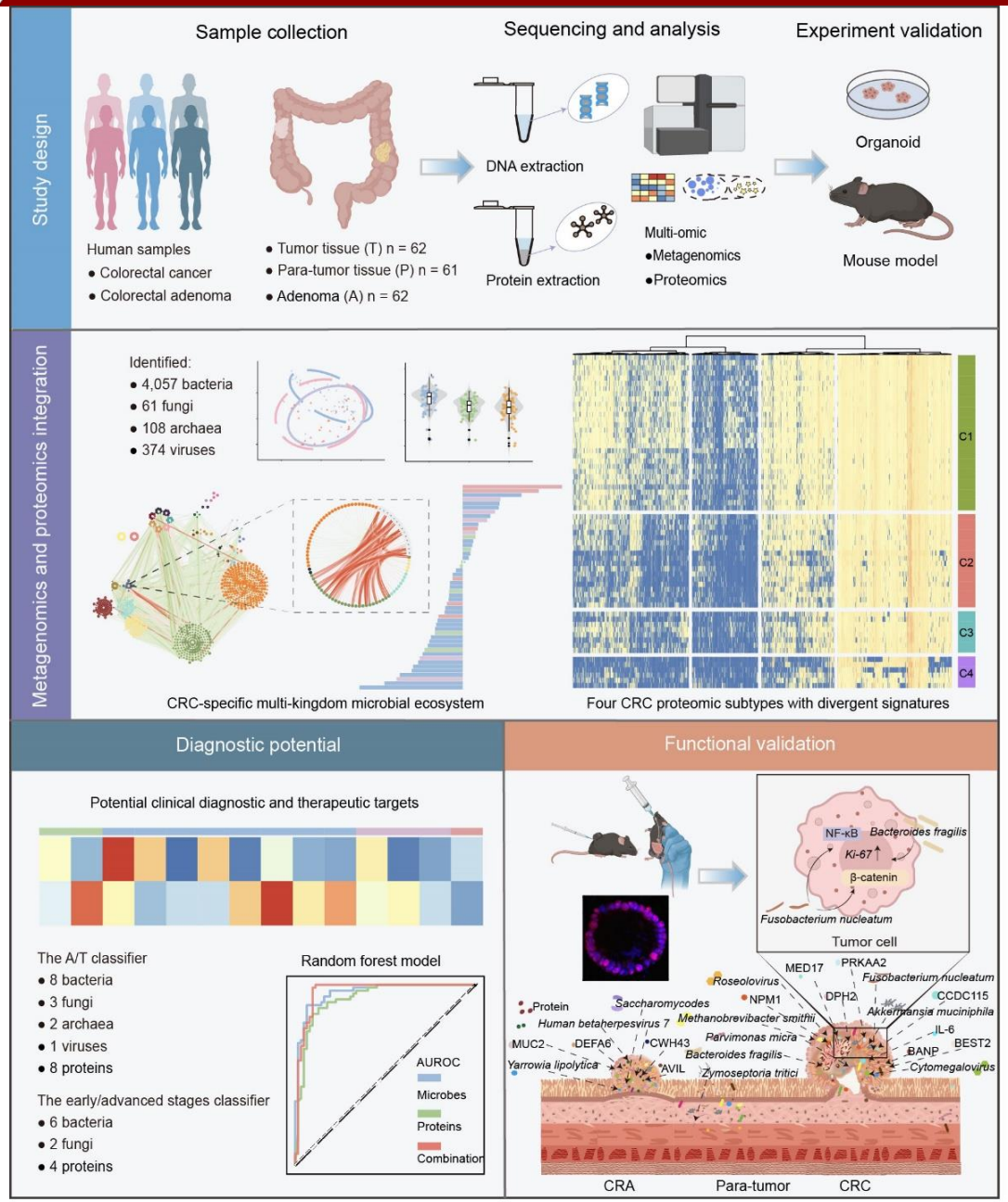

- Integrated metagenomic and proteomic profiling of 185 colorectal tissue samples. and identification of CRC-specific multi-kingdom microbial ecosystems and four molecular subtypes with distinct clinical features.
- Discovery of 14 microbial and 8 protein markers with high diagnostic accuracy for adenoma vs. tumor and early vs. advanced stage classification.
- Functional validation of *Bacteroides fragilis* and *Fusobacterium nucleatum* as key microbial drivers promoting tumor growth via Wnt/β-catenin and NF-κB signaling.
- Insights into dynamic host–microbiome interactions with potential diagnostic and therapeutic relevance.

Fig 1 Schematic overview of this study

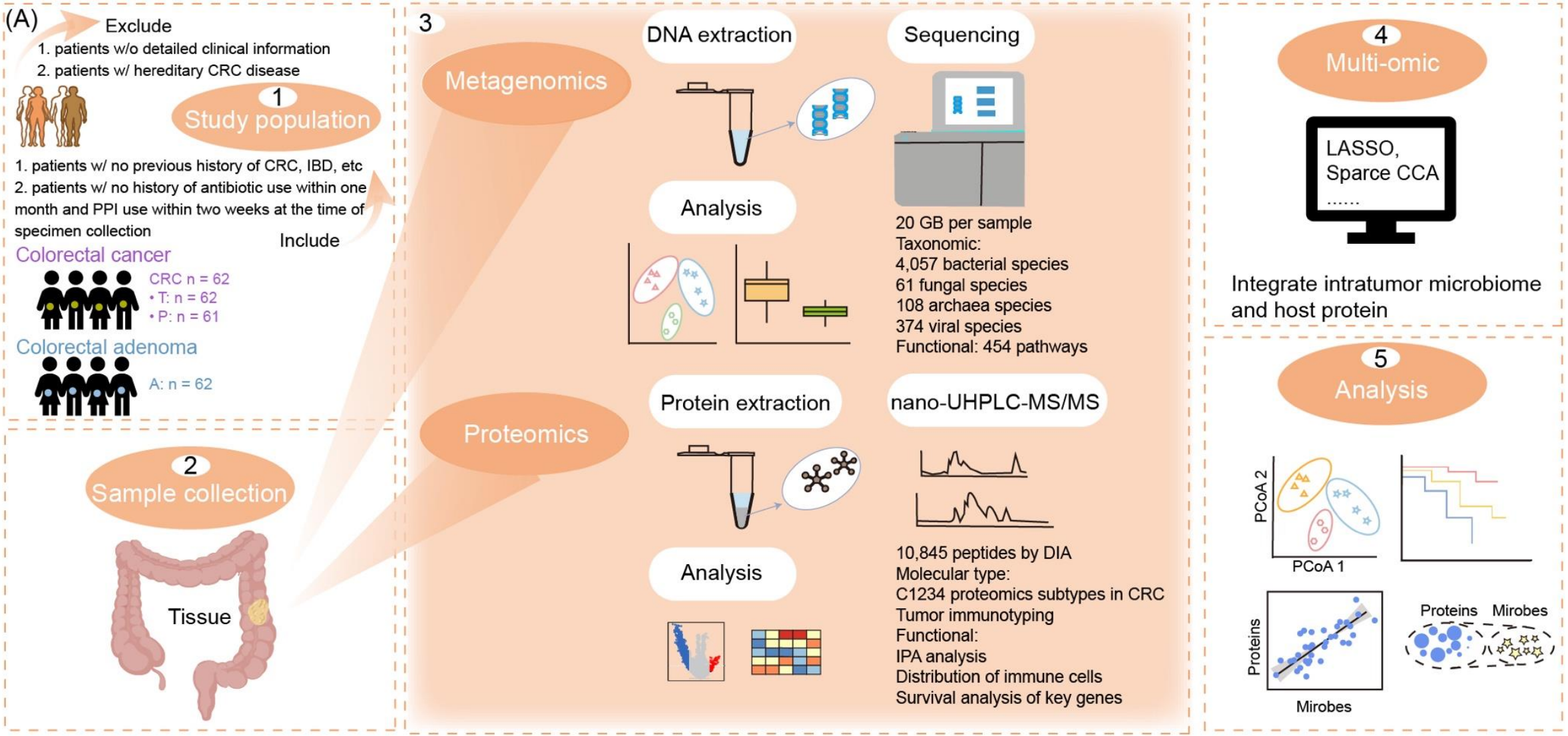

(A) Study design and cohort overview. Integrated metagenomic and proteomic profiling of 185 tissue samples (Adenoma/A, Tumor/T, Para-tumor/P) from 124 patients. Phenotypic data were collected, and analyses compared tissue-resident, gut, and oral microbiomes.

Fig 1 Multi-kingdom microbiome dysbiosis

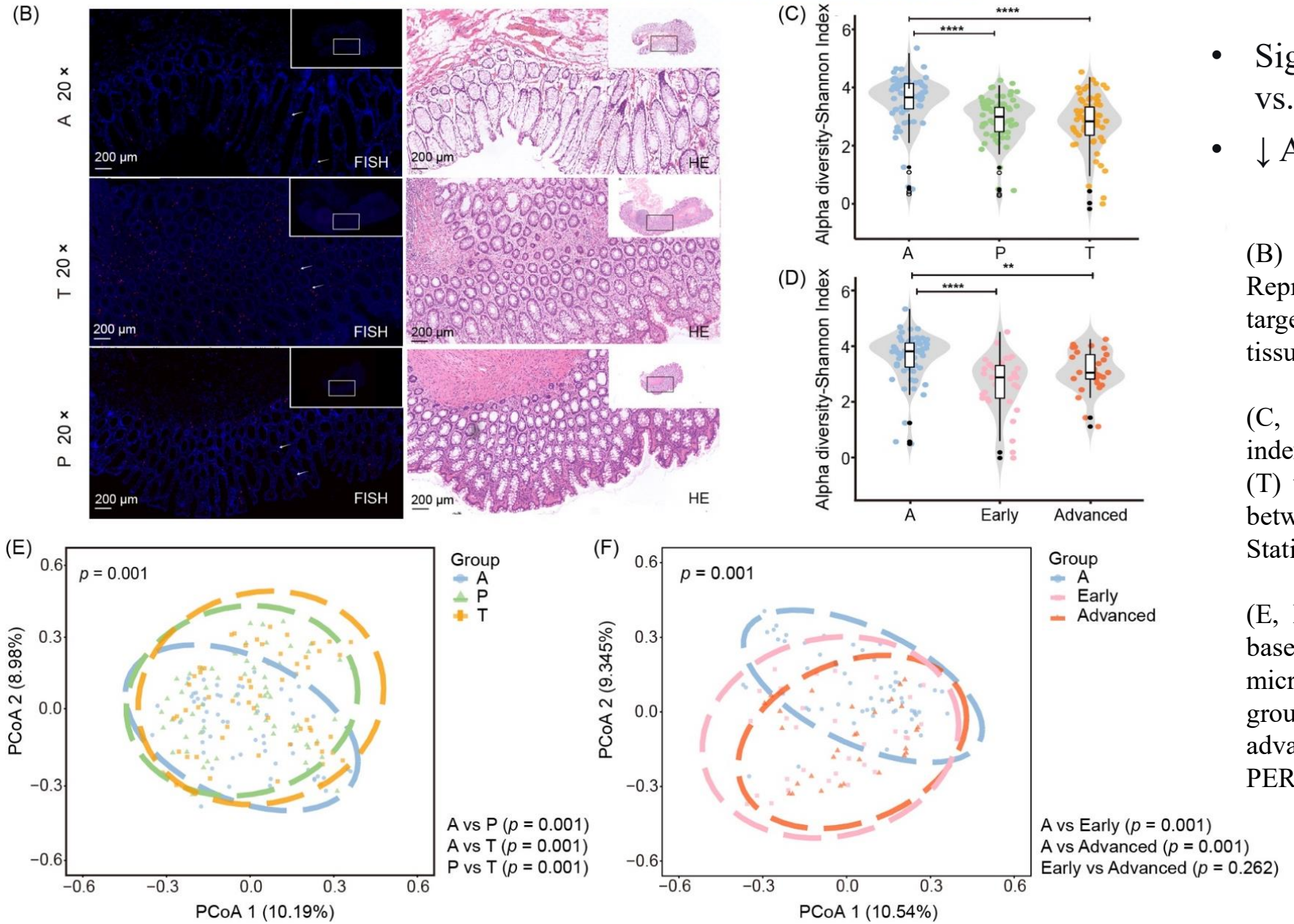

- Significant dysbiosis in tumors (T) vs. adenomas (A).
- ↓ Alpha diversity in T.

(B) Microbial presence validation. Representative H&E staining and FISH targeting fungal 28S rRNA in A, P, and T tissues. Scale bars, 200 μm.

(C, D) Microbial alpha diversity. Shannon index showing significant reduction in tumor (T) versus adenoma (A) tissues (C), but not between early and advanced stages (D). Statistical testing by Kruskal-Wallis test.

(E, F) Microbial beta diversity. PCoA plots based on Bray-Curtis distance reveal distinct microbial communities among A, P, and T groups (E), and between A, early, and advanced groups (F). Statistical testing by PERMANOVA (two-sided).

Fig 2 Multi-kingdom alterations

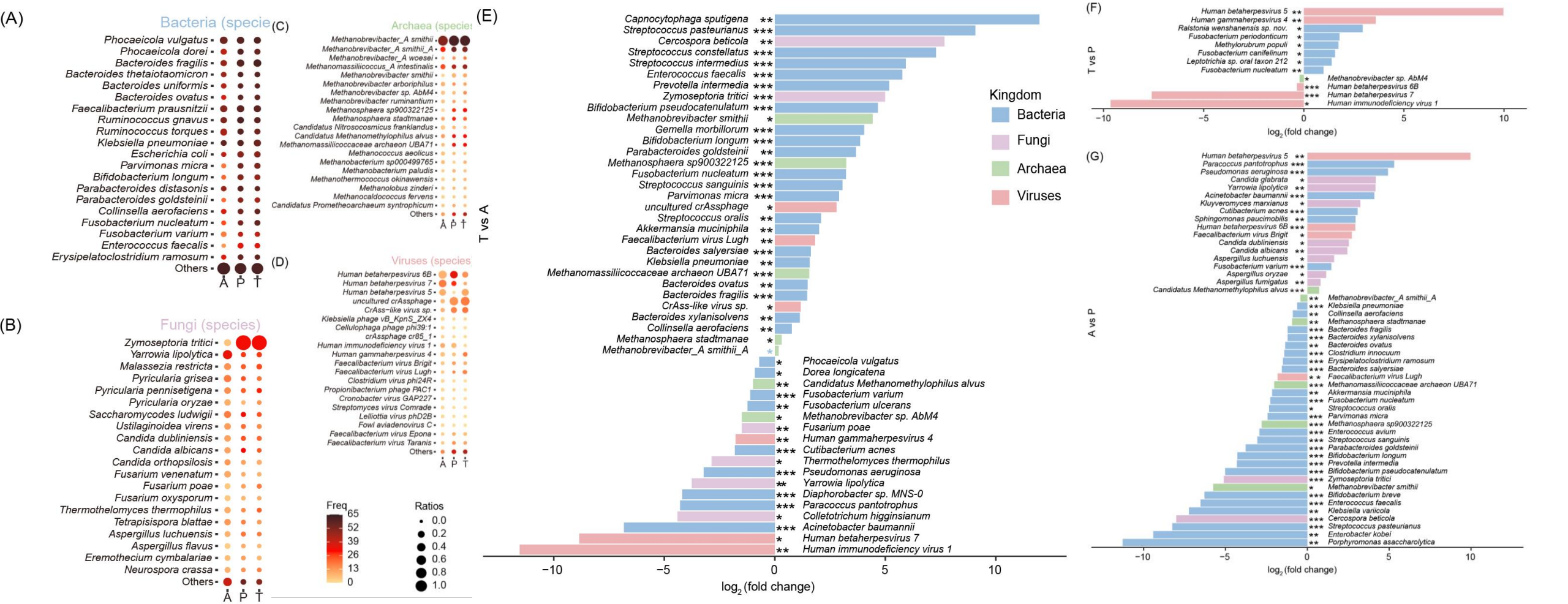

(A-D) Species-level taxonomic composition of the tissue-resident (A) bacteriome, (B) mycobiome, (C) archaeome, and (D) virome across adenoma (A), para-tumor (P), and tumor (T) tissues. Bubble size and color intensity represent relative abundance and prevalence, respectively.

(E-G) Differential abundance analysis of microbial species in paired comparisons: (E) T vs. A, (F) T vs. P, and (G) A vs. P. Points are colored by microbial kingdom. Statistical significance is indicated as $*p < 0.05$, $**p < 0.01$, $***p < 0.001$.

Fig 3 Multi-kingdom microbial interactions and functional associations

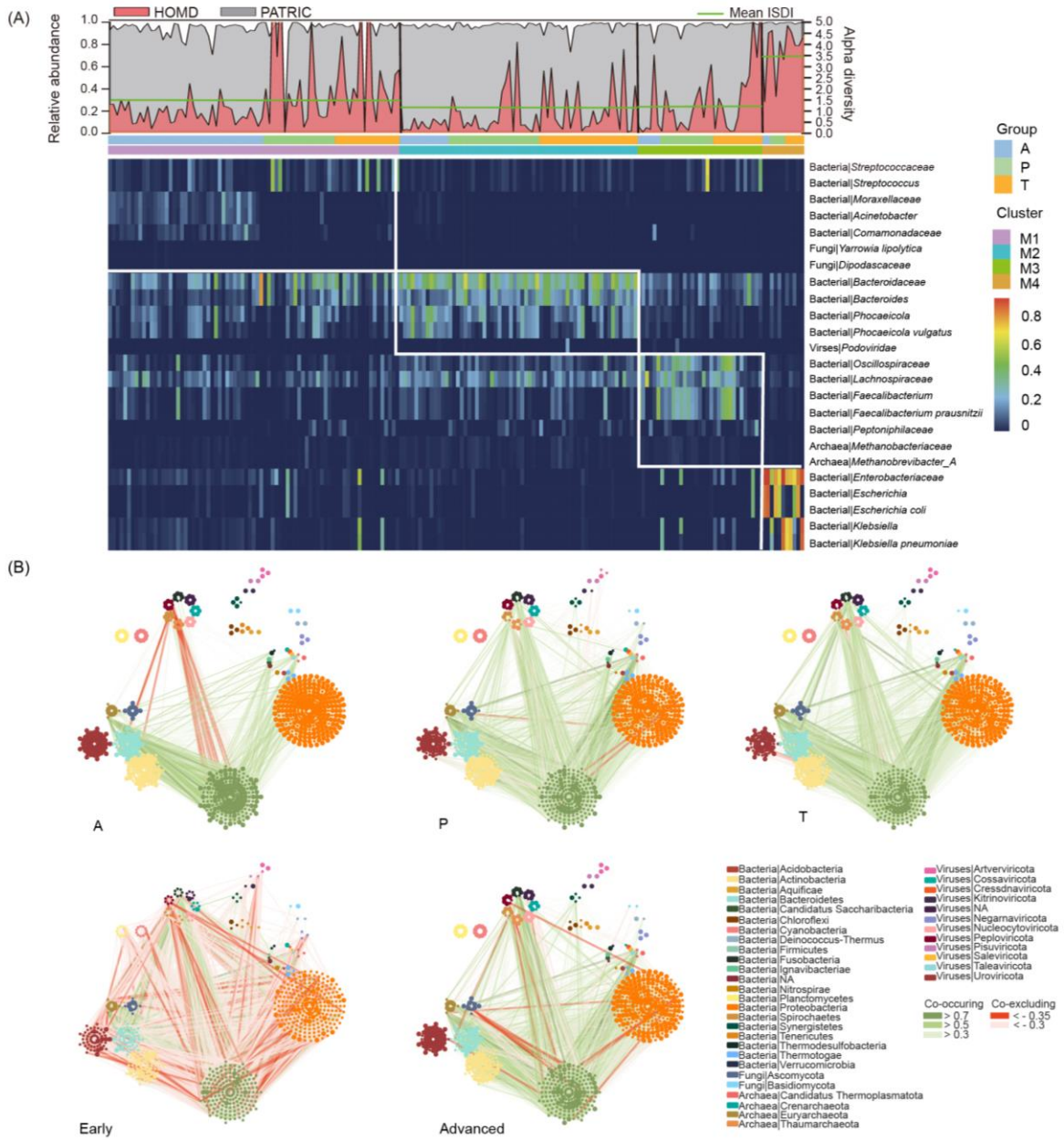

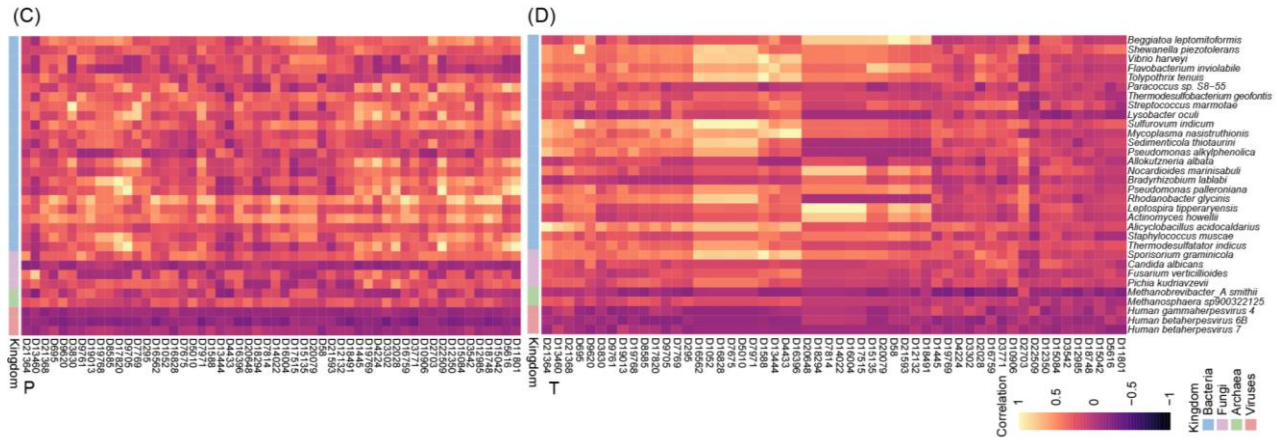

(A) Microbial community clusters (M1-M4) identified by Dirichlet multinomial mixtures (DMM) modeling. Bar plots show the proportion of oral and pathogenic strains within each cluster.

(B) Genus-level microbial interaction networks across sample groups, inferred by SparCC. Node color and size represent taxonomy and abundance, respectively. Edges denote significant correlations (|SparCC| > 0.3; green for positive, red for negative).

(C, D) Heatmaps of Spearman correlations between differential microbial species and metabolic pathways in para-tumor (C) and tumor (D) tissues. Top 50 bacterial and top 10 fungal/archaeal/viral species-pathway pairs are shown.

Fig 4 Proteomic landscape in CRC progression

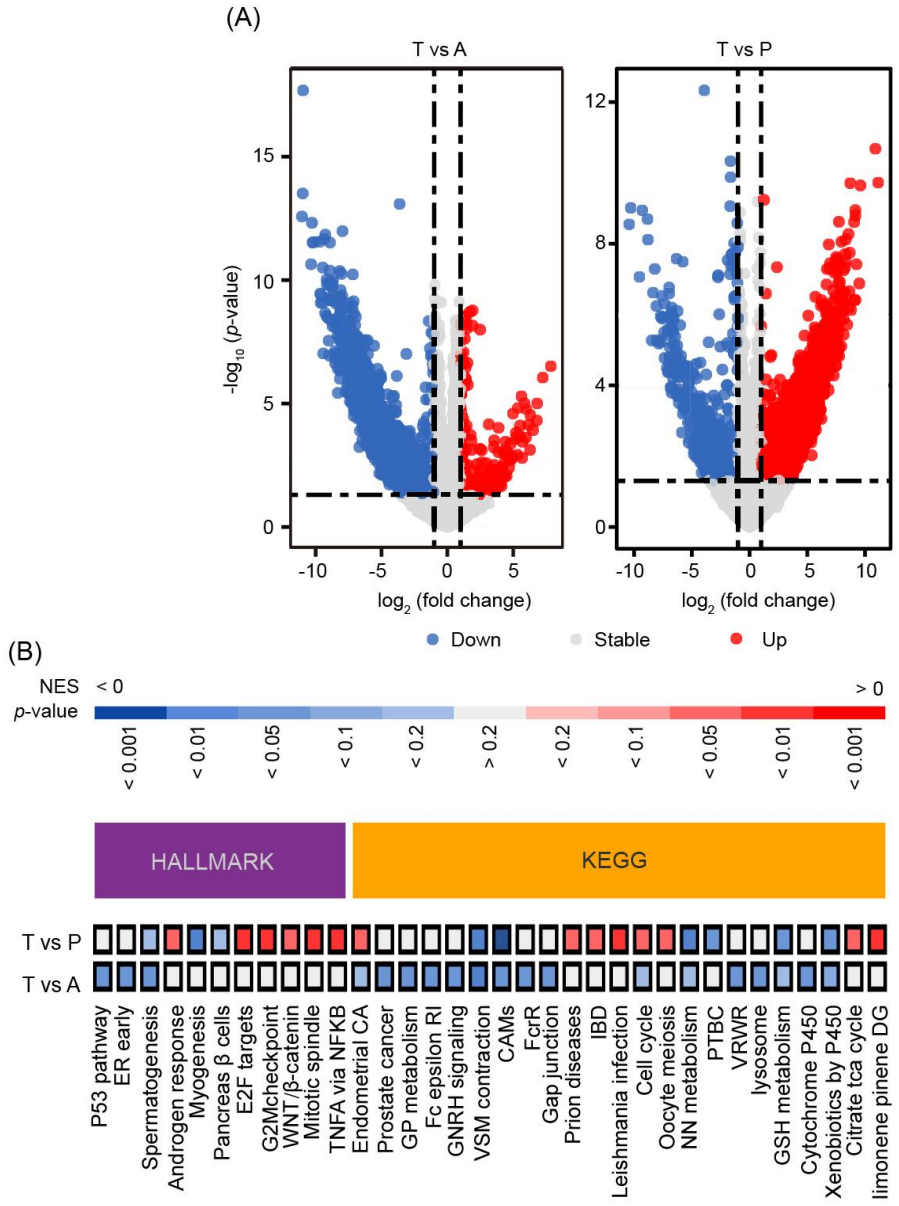

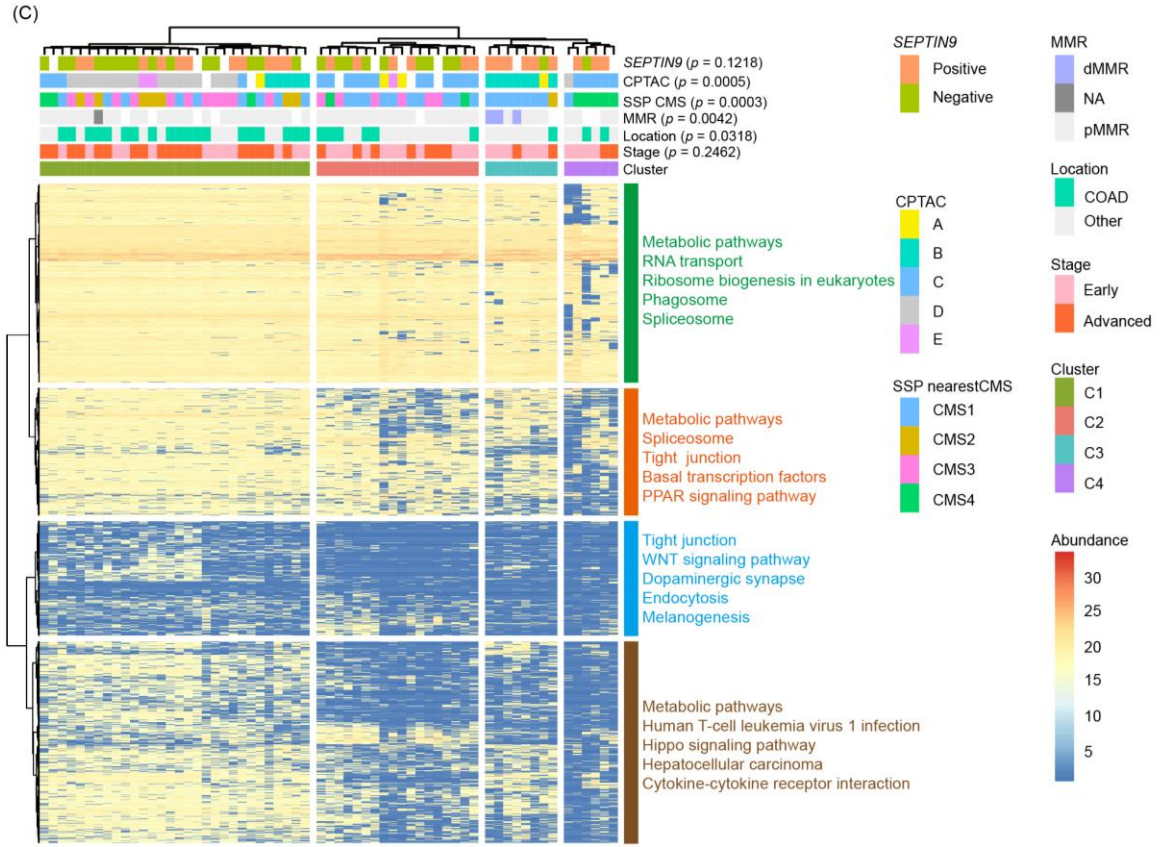

(A) Volcano plots of differentially expressed proteins in tumor (T) versus adenoma (A) and T versus para-tumor (P) tissues. Red and blue points denote up- and down-regulated proteins, respectively.

(B) Gene set enrichment analysis (KEGG and Hallmark) for T vs. P and T vs. A comparisons. Bars indicate normalized enrichment scores (NES).

(C) Consensus clustering of tumor proteomes defines four molecular subtypes (C1–C4). Top annotations indicate clinical and molecular features.

Fig 4 Functional validation of oncogenic pathways

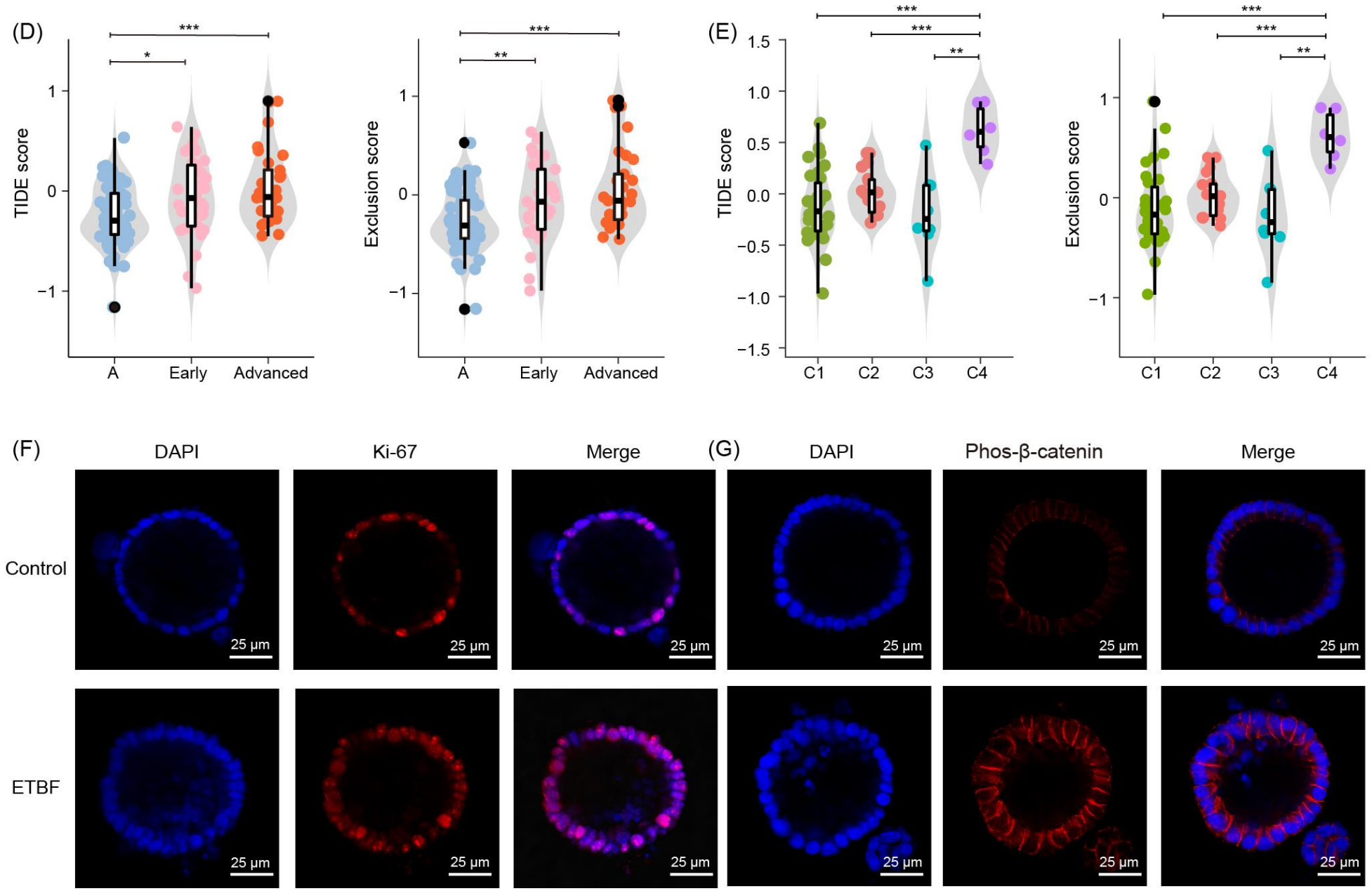

(D, E) Tumor Immune Dysfunction and Exclusion (TIDE) scores across tissue groups (D) and proteomic subtypes (E). Boxplots show median and IQR; two-sided t-test.

(F, G) Representative images of patient-derived organoids co-cultured with enterotoxigenic *Bacteroides fragilis* (ETBF), showing increased proliferation (Ki-67, F) and activation of Wnt/β-catenin signaling (phosphorylated β-catenin, G). Scale bar, 25 μm.

Fig 5 Protein-protein interaction and pathway analysis in tumor tissues

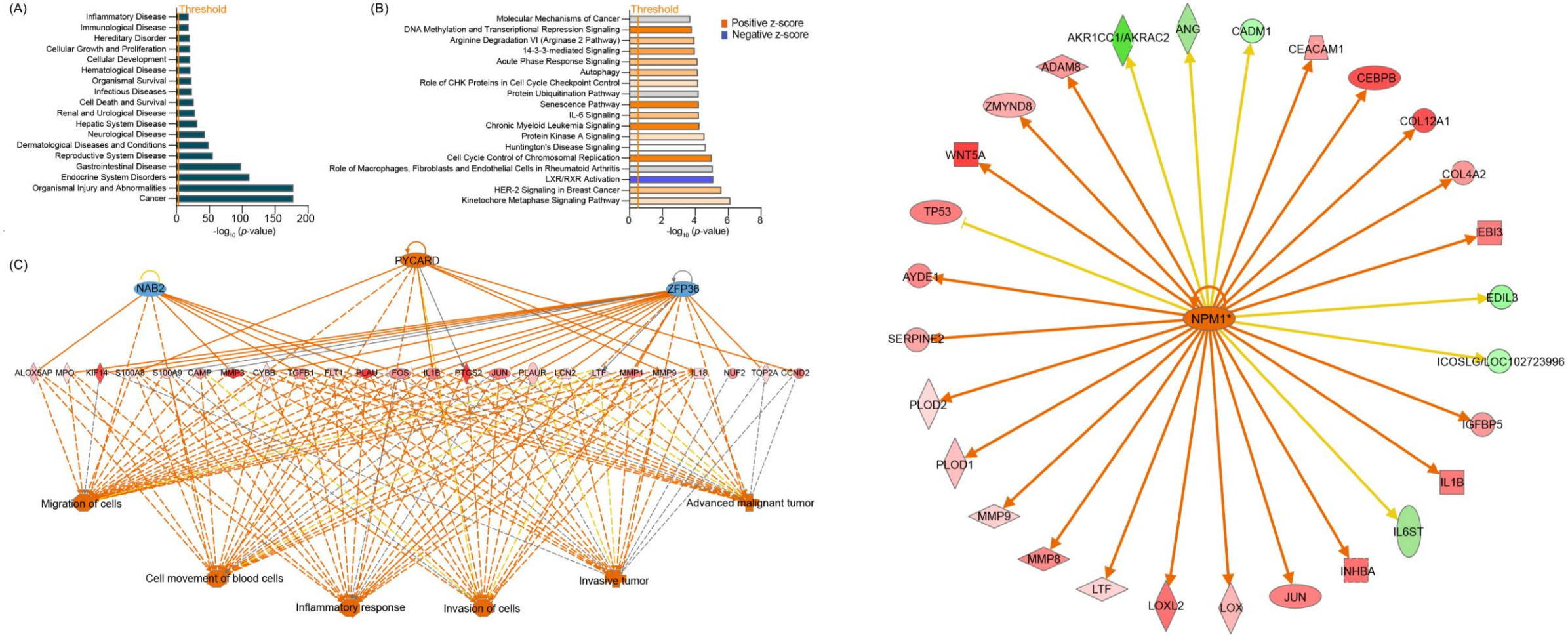

(A) Disease and functional annotation of differentially expressed proteins. Bar length represents -log (*p*-value).

(B) Enrichment of canonical pathways. Orange indicates activation (z-score > 2), blue indicates inhibition (z-score < -2). Significance was determined by Fisher's exact test ($p < 0.05$, $|z\text{-score}| > 2$).

(C) Key protein interaction network. Node color and shading represent the direction and magnitude of protein expression changes.

(D) Upstream regulatory network. Lines indicate predicted regulatory relationships between upstream regulators and target molecules (orange: activation; blue: inhibition).

Fig 6 Shared and specific host–microbiome interactions in CRC progression

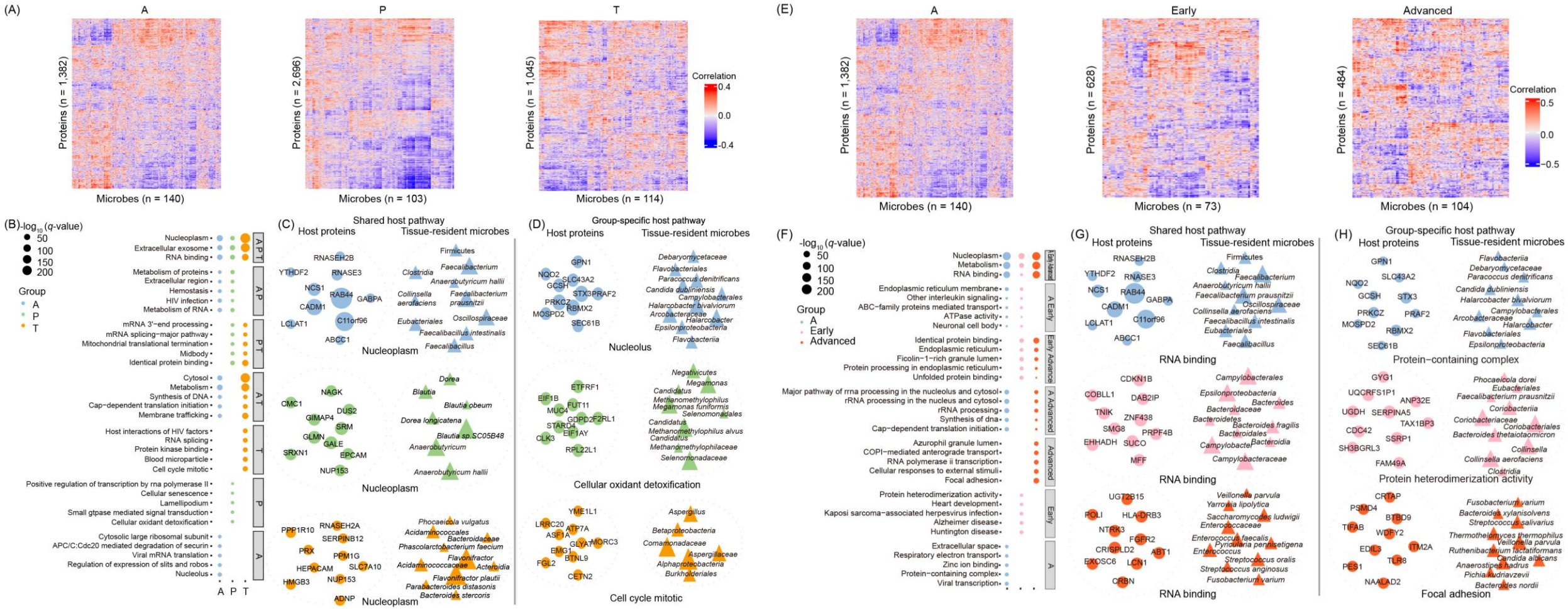

(A, E) Heatmaps of host protein–microbe correlations identified by LASSO regression in adenoma (A), para-tumor (P), and tumor (T) tissues (A), and in adenoma, early-, and advanced-stage tumors (E). FDR < 0.1.

(B, F) Enriched host pathways associated with microbiome composition across tissue types (B) and disease stages (F). Dot size indicates enrichment significance.

(C, D, G, H) Shared (C, G) and group-specific (D, H) host pathway–microbe associations visualized by sparse canonical correlation analysis (CCA). Circle and triangle sizes represent gene and microbe CCA coefficients, respectively.

Fig7 Microbiome-host interactions define CRC-associated mycotypes

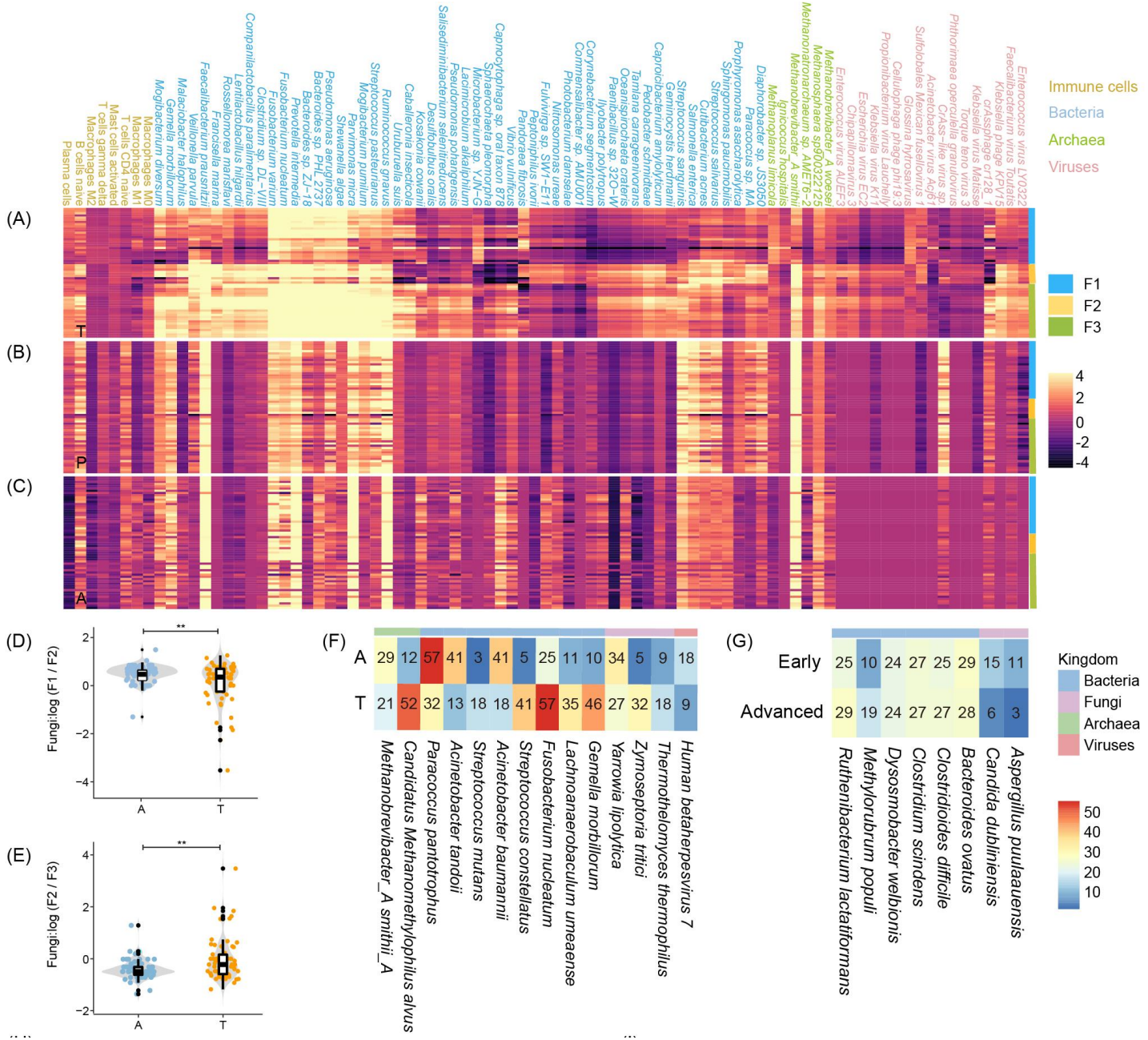

(A–C) Co-occurrence networks of fungi, bacteria, archaea, viruses, and immune cells in tumor (A), para-tumor (B), and adenoma (C) tissues, revealing three fungal-driven “mycotypes” (F1–F3).

(D, E) Log-ratio abundances of mycotype pairs F1/F2 (D) and F2/F3 (E) between adenoma and tumor tissues (two-sided t-test).

(F, G) Feature importance of multi-kingdom microbial markers for distinguishing adenoma from tumor (F) and early- from advanced-stage cancer (G), based on random forest Gini importance.

Fig7 Diagnostic models and functional validation

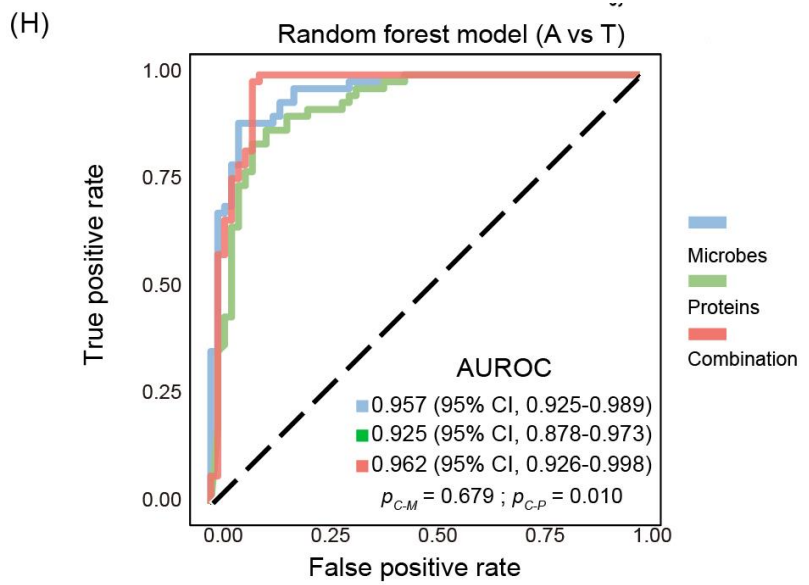

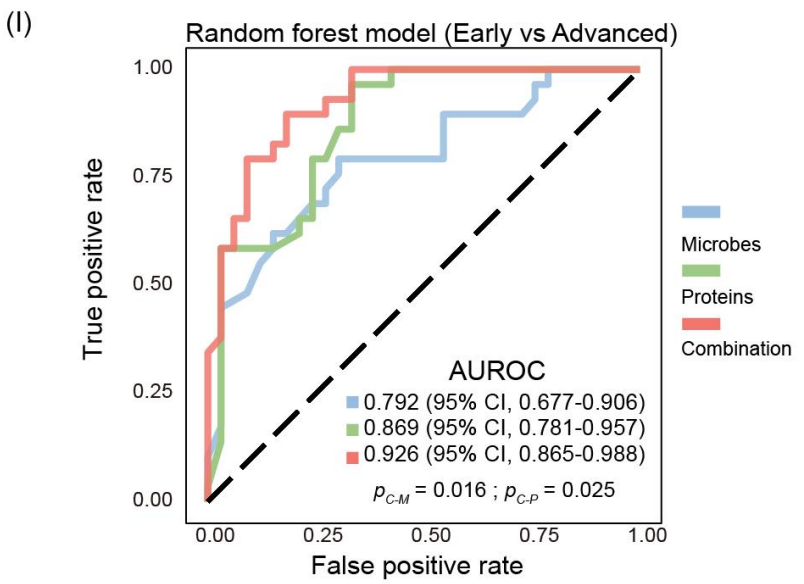

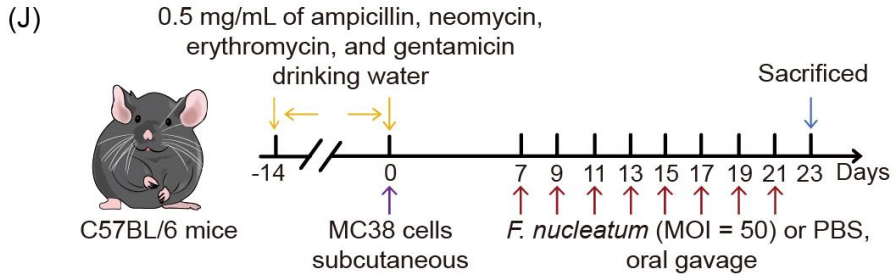

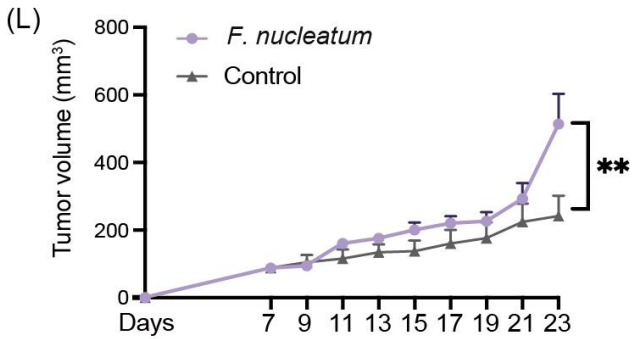

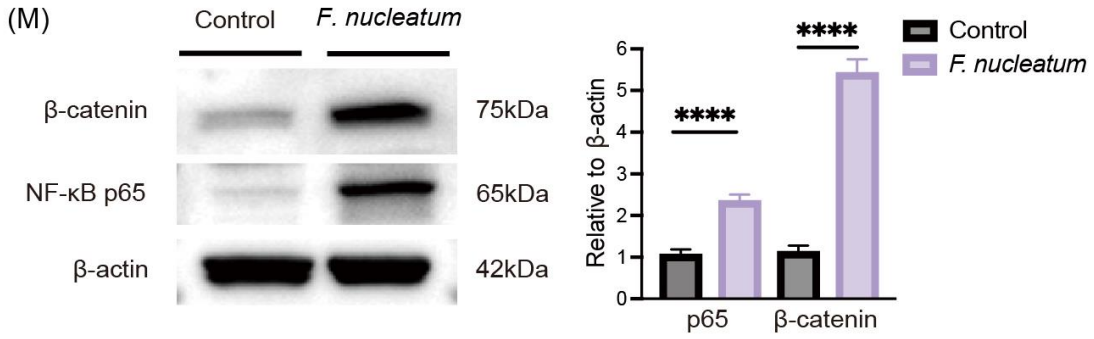

(H, I) ROC curves of random forest models using microbial markers (red), protein markers (green), or their combination (blue) to discriminate adenoma vs. tumor (H) and early vs. advanced stage (I). AUROC values and *p*-values for model comparisons are shown.

(J–M) Fusobacterium nucleatum promotes tumor growth and activates oncogenic pathways in a murine allograft model. Experimental scheme (J), tumor images and growth curves (K, L), and Western blot analysis of β-catenin and NF-κB p65 (M). Data are mean ± SEM; two-way ANOVA (L) or Student's t-test (M). Scale bar, 1 cm.

Summary

- We systematically delineated the dynamic evolution of the multi-kingdom microbiota in CRC and, for the first time, defined immune- and bacteria-associated "mycotypes," uncovering a critical role for fungi in the tumor microenvironment.
- We constructed the first protein-level map of the intratumoral multi-kingdom microbiome-host interaction network, identifying a combinatorial microbial-protein biomarker signature with high diagnostic accuracy for discriminating adenoma from carcinoma and early from late-stage disease.
- Functional validation confirmed that *F. nucleatum* and ETBF promote CRC progression by activating Wnt/β-catenin and NF-κB signaling, providing a mechanistic rationale for developing microbiota-targeted diagnostics and therapies to alleviate the CRC burden.
- Website: https://www.bioincloud.tech/

Di Wu, An-Jun Wang, De-Chao Bu, Yan-Yan Sun, Chen-Hao Li, Yue-Mei Hong, Shan Zhang, et al. 2025. The Interplay Between Tissue-Resident Microbiome and Host Proteins by Integrated Multi-omics During Progression of Colorectal Adenoma to Carcinoma. ***iMeta*** 4: e70090. https://doi.org/10.1002/imt2.70090

iMeta: To be top journals in biology and medicine

WILEY

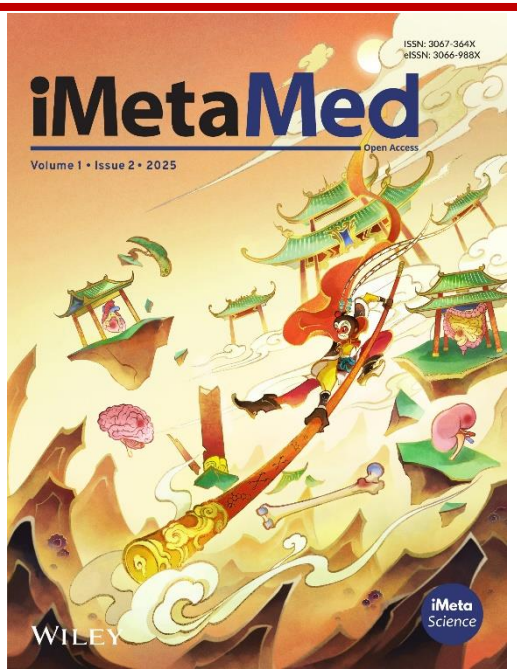

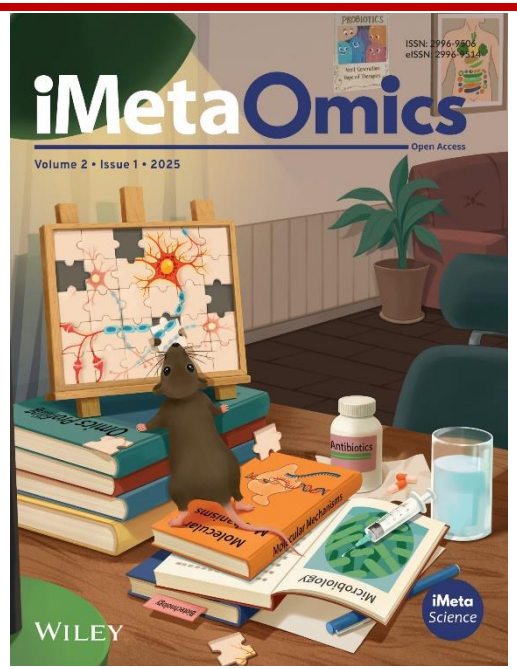

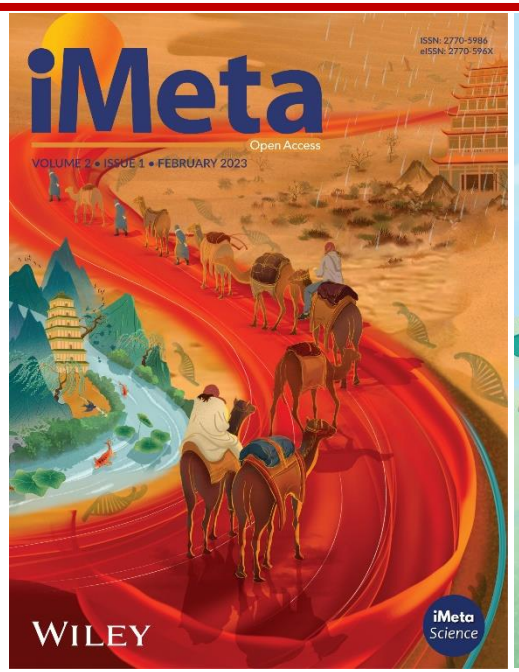

"***iMeta***" launched in 2022 by iMeta Science Society, impact factor (IF) **33.2**, ranking top 65/22249 in world and 2/161 in the microbiology. It aims to publish innovative and high-quality papers with broad and diverse audiences. **Its scope is similar to *Cell*, *Nature Biotechnology/Methods/Microbiology/Medicine/Food***. Its unique features include video abstract, bilingual publication, and social media with 600,000 followers. Indexed by **SCIE/ESI**, **PubMed**, **Google Scholar** etc.

"***iMetaOmics***" launched in 2024, with a **target IF>10, and its scope is similar to *Nature Communications*, *Cell Reports***, *Microbiome, ISME J, Nucleic Acids Research, Briefings in Bioinformatics,* etc.

"***iMetaMed***" launched in 2025, with a **target IF>15, similar to *Med, Cell Reports Medicine*, *eBioMedicine, eClinicalMedicine*** etc.

Society: http://www.imeta.science
Publisher: https://wileyonlinelibrary.com/journal/imeta

Submission: iMeta: https://wiley.atyponrex.com/journal/IMT2
iMetaOmics: https://wiley.atyponrex.com/journal/IMO2
iMetaMed: https://wiley.atyponrex.com/journal/IMM3

iMetaScience
iMetaScience

office@imeta.science
imetaomics@imeta.science

Promotion Video

Update 2025/7/6